Eigenvalue spectrum of the product of transfer matrices for directed polymers

(Dated: November 27, 2024)

Abstract

Abstract.

In Chapter 1, we saw that the KPZ universality class is characterized by fluctuations which obey TW statistics. In particular, this result has been derived analytically for the free energy in the DPRM model using a replica Bethe ansatz method [1–3]. We discussed also that the TW probability distributions originate from the mathematical study of Gaussian random matrices, and more specifically, from the study of their eigenvalue spectra. In this chapter, we turn to a mathematical analysis of the transfer matrix formulation of DPRM in order to explore this connection on the level of matrices. Similar questions have been considered in the context of disordered elastic networks, where each transfer matrix contains information about the propagation of the displacement field [4]. Our interest in the eigenvalue spectrum of the product of DPRM transfer matrices is physically motivated by systems of non-intersecting paths, a problem which has been studied extensively in the context of the commensurate-incommensurate transition [5, 6].

To simplify the analysis, we construct a set of transfer matrices in such a way that ensures all eigenvalues of the product matrix are real and positive. We compute the fluctuations in the spectrum, and find similarities in distribution to Gaussian random matrices for all eigenvalues. The spacing between eigenvalues is also relevant for a finite density of non-intersecting DPRMs, as it determines the cost associated with adding more such directed polymers in a grand canonical setting. Compared to the pure system, the presence of disorder changes the scaling of the spacing near the largest eigenvalue from $1/N^2$ to $1/N$, where N is the system size, thus changing the density of states.

For a DPRM system of size N, let $\tilde{Z}(x_0, x, t)$ denote the partition function of a directed polymer originating from $(x_0, 0)$ and terminating at (x, t), with $x_0, x \in [1, \ldots, N]$ and $t > 0$. Using the transfer matrix formulation, $\tilde{Z}(x_0, x, t)$ can be written recursively in terms of the partition functions at time $t - 1$,

$$\tilde{Z}(x_0, x, t) = \sum_{x'} \langle x|\mathbf{T}(t)|x'\rangle \tilde{Z}(x_0, x', t-1). \tag{1}$$

If we define the product of transfer matrices,

$$\mathbf{W}(t) = \prod_{t'=1}^{t} \mathbf{T}(t'). \tag{2}$$

we can rewrite the partition function as

$$\tilde{Z}(x_0, x, t) = \langle x|\mathbf{W}(t)|x_0\rangle. \tag{3}$$

We consider the ensemble of directed polymers whose endpoints are fixed to be at the same spatial position x. Summing over all such paths then gives the partition function

$$Z(t) = \sum_{x=1}^{N} \tilde{Z}(x, x, t) = \mathrm{tr}\mathbf{W}(t). \tag{4}$$

The free energy is

$$f = -\frac{\ln Z}{t} = -\frac{\ln[\mathrm{tr}\mathbf{W}(t)]}{t} \simeq -\frac{\ln \lambda_1(t)}{t}, \tag{5}$$

where $\lambda_1(t)$ is the largest eigenvalue of the product matrix $\mathbf{W}(t)$ which dominates the trace. This motivates the definition of the quantity of interest,

$$\epsilon_i(t) = \frac{\ln \lambda_i(t)}{t}, \tag{6}$$

where $\lambda_i(t)$ is the ith largest eigenvalue of the product matrix $\mathbf{W}(t)$.

I. NON-INTERSECTING PATHS

We motivate the study of the quantities ϵ_i, related to the eigenvalue spectrum of the DPRM product matrix, by examining their role in a system of non-intersecting DPRMs [6]. Physical examples include magnetic domain walls in Ising models [7, 8], and pinned flux lines in superconductors [9]. In such systems, if it is favourable to create one domain wall or flux line, it is natural to ask why an infinite number is not created. As we explain below, this is a consequence of the non-crossing condition. The more general problem of non-intersecting paths is also found in the adsorption of an atomic monolayer on a crystalline surface [5, 10–12], and the equilibrium shapes of crystals [13, 14]. The statistical behaviour is exemplified by the commensurate-incommensurate transition, a topic which has sparked much theoretical interest [5, 15–17].

In the pure case (without disorder), the grand canonical free energy $\mathcal{F}$ is obtained by minimizing the following expression over the density r of non-intersecting paths, [5]

$$\frac{\mathcal{F}(r)}{Nt} = f_1 r + b r^3. \tag{7}$$

Using the language of domain walls, N and t are the system dimensions, f_1 is the free energy of a single wall, and $b > 0$ is a constant. The first term, proportional to the density, is intuitive. The second term represents an effective repulsion due to the non-crossing

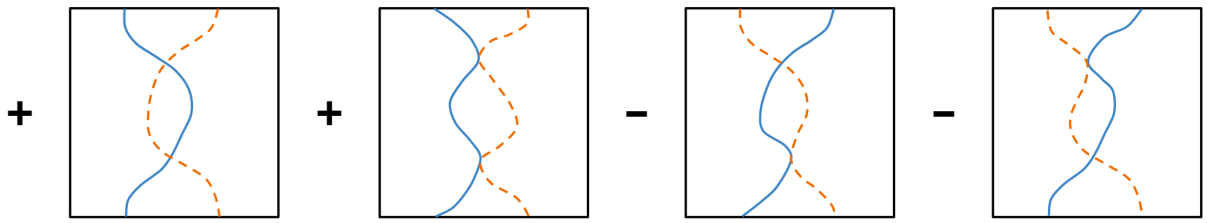

FIG. 1: Illustration of configurations of two DPRMs (solid and dashed lines) which do not satisfy the non-crossing condition. Introducing the factor $(-1)^{\#\text{ of crossings}}$ leads all such terms to cancel.

restriction. Performing the minimization over r, we see that for $f_1 > 0$, no domain walls are formed ($r = 0$). On the other hand, for $f_1 < 0$, a finite density ($r > 0$) of domain walls are added in such a way that the free energy gain is balanced by the entropy loss from imposing the non-crossing condition. These walls can also be interpreted as world-lines of 1D fermions, an approach taken by Pokrovsky and Talapov in Ref. [5].

If we now consider the presence of quenched impurities, the domain walls can be represented by a system of non-intersecting DPRMs. Using the replica Bethe ansatz, the quantity to be minimized over in Eq. 7 becomes [6]

$$\frac{\langle \mathcal{F}(r) \rangle}{Nt} = \langle f_1 \rangle r + br^2, \tag{8}$$

where the angular brackets denote averaging over the disorder, and again, $b > 0$. The effective repulsion term in this case is proportional to r^2 rather than r^3. For the pure system, this repulsion relates to the typical distance between "collisions" of domain walls due to transverse wanderings, whereas for the disordered system, it relates to effects of confinement on a finite density of optimal paths.

In writing down the grand canonical description of DPRM, the key difficulty lies in the implementation of the non-crossing condition. We use the same trick which proved powerful in the Ising problem, of removing the non-crossing condition, and introducing a factor of $(-1)^{\#\text{ of crossings}}$ for each term in the partition function. The terms describing intersecting paths or shared bonds then cancel, as shown in Fig. 1, leaving only contributions from non-crossing configurations.

The grand canonical partition function $\mathcal{Z}$ can then be written in terms of the canonical

partition functions Z_n for n DPRMs.

$$\begin{aligned}\mathcal{Z} &= \exp\left\{\sum_{n=1}^{N}\frac{(-1)^{n+1}}{n}Z_n\right\}\\ &= \exp\left\{\sum_{n=1}^{N}\frac{(-1)^{n+1}}{n}\mathrm{tr}\mathbf{W}^n\right\}\\ &= \exp\left\{\sum_{i=1}^{N}[\ln(1+\lambda_i)]\right\}\\ &= \exp\left\{\sum_{i=1}^{N}\left[\ln\left(1+e^{\epsilon_i t}\right)\right]\right\}. \end{aligned} \tag{9}$$

(One could introduce a chemical potential ν such that $Z_n \to e^{\nu t n} Z_n$ counts the number of added steps. However, without loss of generality, ν can be absorbed into the parametrization of the energies.) In the limit of large t, only terms with $\epsilon_i > 0$ in Eq. 9 will contribute to the free energy,

$$\mathcal{F} = -\frac{\ln \mathcal{Z}}{t} \xrightarrow{t\to\infty} -\sum_{\epsilon_i>0}\epsilon_i. \tag{10}$$

The condition on ϵ_i reflects a constraint on the strength of the average disorder compared to the hopping energy, in order for it to be energetically favourable to create more directed polymers. The value of ϵ_1 determines whether a single DPRM is favourable; after that, the difference $\epsilon_i - \epsilon_{i+1}$ becomes relevant for adding subsequent DPRMs. We can interpret this as filling levels $-\epsilon_i$ in an energy band, starting from $-\epsilon_1$, up to the Fermi energy. The resistance to adding more non-intersecting DPRMs is therefore related to the density of states near the edge of the spectrum.

II. CONNECTION TO RANDOM MATRIX THEORY

It has been well-established both indirectly through the Cole-Hopf transformation, [18] and directly through replica Bethe ansatz solutions, [1–3] that the DPRM free energy in Eq. 5 obeys TW statistics, with the details dependent on the geometry. In the case of Eq. 4, however, the geometry is not strictly pt-pt or pt-line (defined in Chapter 1.2.1). Rather, $Z(t)$ is the sum of an ensemble of pt-pt paths. Thus we expect the limiting distribution to be very similar to TW, but perhaps not precisely the GOE or GUE form. In other words, we can write

$$\epsilon_1(t) = c_0 + c_1 t^{-2/3}\xi, \tag{11}$$

where ξ is an $\mathcal{O}(1)$ random variable whose distribution is TW-like in the limit of large t, and c_0, c_1 are system-specific constants. It is important to note that the regime relevant to DPRM requires $1 \ll t \ll N^{3/2}$, where N is the system size. This scaling constraint stems from the dynamic exponent which governs the KPZ universality class, and ensures that the scalings are not affected by finite size.

In comparison, we consider an $n \times n$ GOE matrix $\mathbf{L}$ with i.i.d. elements $L_{ii} \sim \mathcal{N}(0, 2/n)$, $L_{ij} = L_{ji} \sim \mathcal{N}(0, 1/n)$ [or respectively, GUE matrix $\mathbf{M}$ with i.i.d. elements $M_{ii} \sim \mathcal{N}(0, 1/n)$, $M_{ij} = \overline{M_{ji}} \sim \mathcal{N}(0, 1/2n) + i\mathcal{N}(0, 1/2n)$]. The largest eigenvalue then has the following scaling form [19, 20],

$$\lambda_1^{\mathrm{TW}}(n) = 2 + n^{-2/3}\xi, \tag{12}$$

where ξ is a TW-GOE (TW-GUE) random variable in the limit of large n.

The similarities between $\epsilon_1(t)$ in Eq. 11 and $\lambda_1^{\mathrm{TW}}(n)$ in Eq. 12 are immediately evident. The time t [also number of transfer matrices in the product matrix $\mathbf{W}(t)$] in the DPRM context appears to play an analogous role to the matrix size n in the GOE and GUE context. We compare numerics for the DPRM product matrix with known results from random matrix theory in Section V, and explore whether the connection extends beyond the scaling forms of the largest eigenvalue.

III. DEFINITION OF THE TRANSFER MATRIX

We define the DPRM transfer matrix at time t as

$$\mathbf{T}(t) = \begin{pmatrix} \eta_1(t) & \gamma & 0 & \cdots & 0 \\ \gamma & \eta_2(t) & \gamma & \cdots & 0 \\ 0 & \gamma & \eta_3(t) & \cdots & 0 \\ \vdots & \vdots & \vdots & \ddots & \vdots \\ 0 & 0 & 0 & \cdots & \eta_N(t) \end{pmatrix}, \tag{13}$$

where $\eta_i(t) = \exp[-\varepsilon_i(t)]$ are i.i.d. random variables on the main diagonal, with constant elements $\gamma > 0$ on the off-diagonals. We choose $\varepsilon_i(t) \in \mathcal{U}(\mu, \sigma^2)$, uniformly distributed with mean μ and variance σ^2. For mathematical reasons explained in section V, the parameters are constrained by the relation

$$\mu + \sqrt{3}\sigma < -\ln(2\gamma), \tag{14}$$

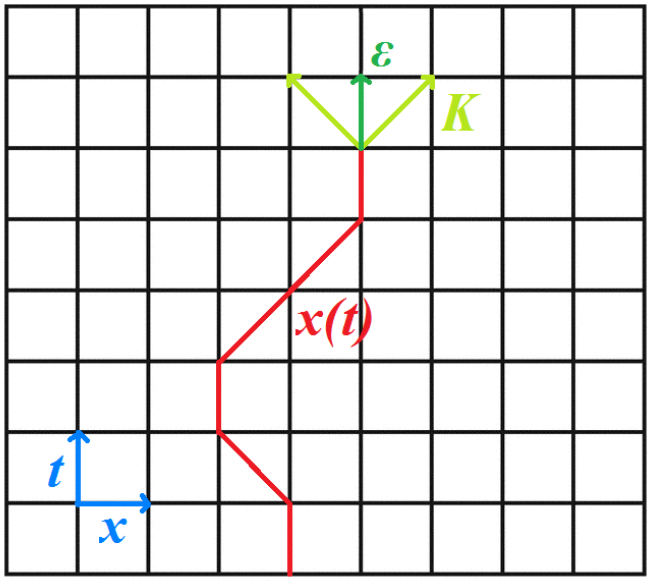

FIG. 2: Illustration of the DPRM geometry described by the transfer matrix in Eq. 13. For a directed polymer $x(t)$, propagating forwards is associated with a random energy ε, while deviating to the left or right is associated with a hopping energy K.

which ensures $\eta_i(t) > 2\gamma$, $\forall i$ and $\forall t$.

The above transfer matrix describes DPRM on a square lattice with closed boundary conditions. At each time t, the path at position i may propagate forward, picking up a random energy $\varepsilon_i(t)$, or deviate to the left or right, picking up a hopping energy $K = -\ln\gamma$ (see Fig. 2).

The details of the model are chosen to ensure that all eigenvalues λ_i of the product matrix $\mathbf{W}$ are real and positive (see section V for a detailed proof). This allows us to study the objects of interest, $\epsilon_i = \ln\lambda_i/t$, which would otherwise be ill-defined. Note that the condition $\lambda_i \in \mathbb{R}^+$ is not a trivial one. Although an individual transfer matrix $\mathbf{T}$ is real, positive, and symmetric, there is a different realization of randomness for each time t. Thus the product matrix $\mathbf{W}$ is in general, real and positive, but not symmetric. The Perron-Fröbenius theorem guarantees that the largest eigenvalue is unique and real (positive), but *a priori*, all other eigenvalues need not be real. Indeed, for other geometries of DPRM, the spectrum is in general composed of many complex conjugate pairs of eigenvalues, the physical significance of which is unclear.

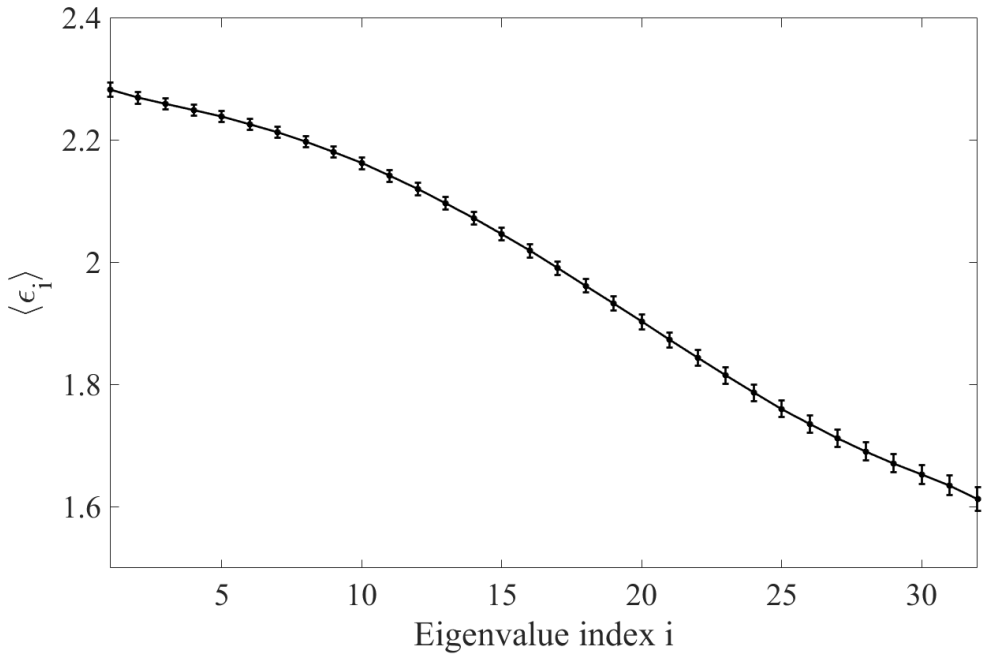

FIG. 3: Average eigenvalue spectrum for the product of DPRM transfer matrices $\mathbf{W}$ with parameters $t = 32$ and $N = 32$. The data points indicate the mean of $\epsilon_i = \ln \lambda_i / t$, where λ_i is the ith largest eigenvalue of $\mathbf{W}$, and the errorbars indicate the standard deviation.

IV. STATISTICS OF THE EIGENVALUE SPECTRUM

Armed with the above definition, we analyze the complete spectrum of the product of transfer matrices. We compute numerically the eigenvalues λ_i of $\mathbf{W}$, with parameters $t = 32$ and $N = 32$, over 2^{25} realizations (the scaling of fluctuations is computed over 2^{22} realizations instead). We choose $\mu = -2$ and $\sigma^2 = 1/12$ for the random energies, and $\gamma = 1$ for the hopping energies. The mean values of $\epsilon_i = \ln \lambda_i / t$ are plotted in Fig. 3, with errorbars indicating the respective standard deviations.

A. Probability distributions

We focus on the distributions of ϵ_i after appropriate rescaling of the the mean and variance. From Eq. 11, we expect ϵ_1, corresponding to the largest eigenvalue of $\mathbf{W}$, as well as the DPRM free energy, to obey TW-like statistics. This is indeed confirmed in Fig. 4a. Rather surprisingly however, we find that ϵ_N, corresponding to the smallest eigenvalue of

W, also has the same TW-like distribution. This is especially remarkable given the discrepancy in the variances (see Fig. 3). Nevertheless, it is reminiscent of the symmetry known to exist in Gaussian random matrices, between the pairs of eigenvalues λ_i^{TW} and $\lambda_{N+1-i}^{\mathrm{TW}}$. There, the behaviour is dictated by the symmetry of the Wigner semicircle distribution $[\rho(\lambda) = \sqrt{4-\lambda^2}/2\pi]$ for the overall spectrum [21]. The study of non-intersecting DPRMs in section I provides some physical intuition for the correspondence observed between pairs ϵ_i and ϵ_{N+1-i}. Since the quantity ϵ_i is related to creating i directed paths, it could, conversely, be interpreted as creating $N-i+1$ empty "paths".

Numerically, this pairwise correspondence persists beyond the extremal eigenvalues for the DPRM product matrix as well. In fact, for any i, the pair ϵ_i and ϵ_{N+1-i} shares the same distribution not only with each other, but also with the analogous eigenvalue pair for Gaussian random matrices. For instance, in Fig. 4b, we see that $\epsilon_{N/2}$ and $\epsilon_{N/2+1}$ are Gaussian in distribution, mirroring the expectation for bulk eigenvalues in GOE and GUE matrices [22, 23]. The distribution of the remaining eigenvalues interpolate between TW near the edge of the spectrum, and Gaussian in the bulk.

B. Scaling of fluctuations

We compute also the scaling exponents for fluctuations of individual eigenvalues. For Gaussian random matrices, the following rigidity estimate exists [24, 25],

$$\mathrm{Var}[\lambda_i^{\mathrm{TW}}(n)] \sim n^{-4/3}[\min\{i, n+1-i\}]^{-2/3}. \tag{15}$$

For the extremal eigenvalues λ_1^{TW} and λ_n^{TW}, the scaling of fluctuations reduces to $n^{-2/3}$, consistent with Eq. 12; for the bulk eigenvalues, however, this scaling is n^{-1}. The term rigidity refers to an effective repulsion between consecutive eigenvalues, specifically in comparison to i.i.d. random variables drawn from the same Wigner semicircle distribution. In the latter case, order statistics yield typical fluctuations of order $n^{-1/2}$ instead [25]. We plot the analogous scaling exponents for the DPRM product matrix in Fig. 5. For ϵ_1 related to the DPRM free energy, we find $[\mathrm{Var}(\epsilon_1)]^{1/2} \sim t^{-2/3}$, as expected from Eq. 11. However, for ϵ_i in the bulk, the scaling is approximately $t^{-1/2}$, consistent with ordered i.i.d random variables rather than GOE or GUE eigenvalues. The correspondence between pairs of eigenvalues observed earlier in the probability distributions is also present in the scaling of fluctuations,

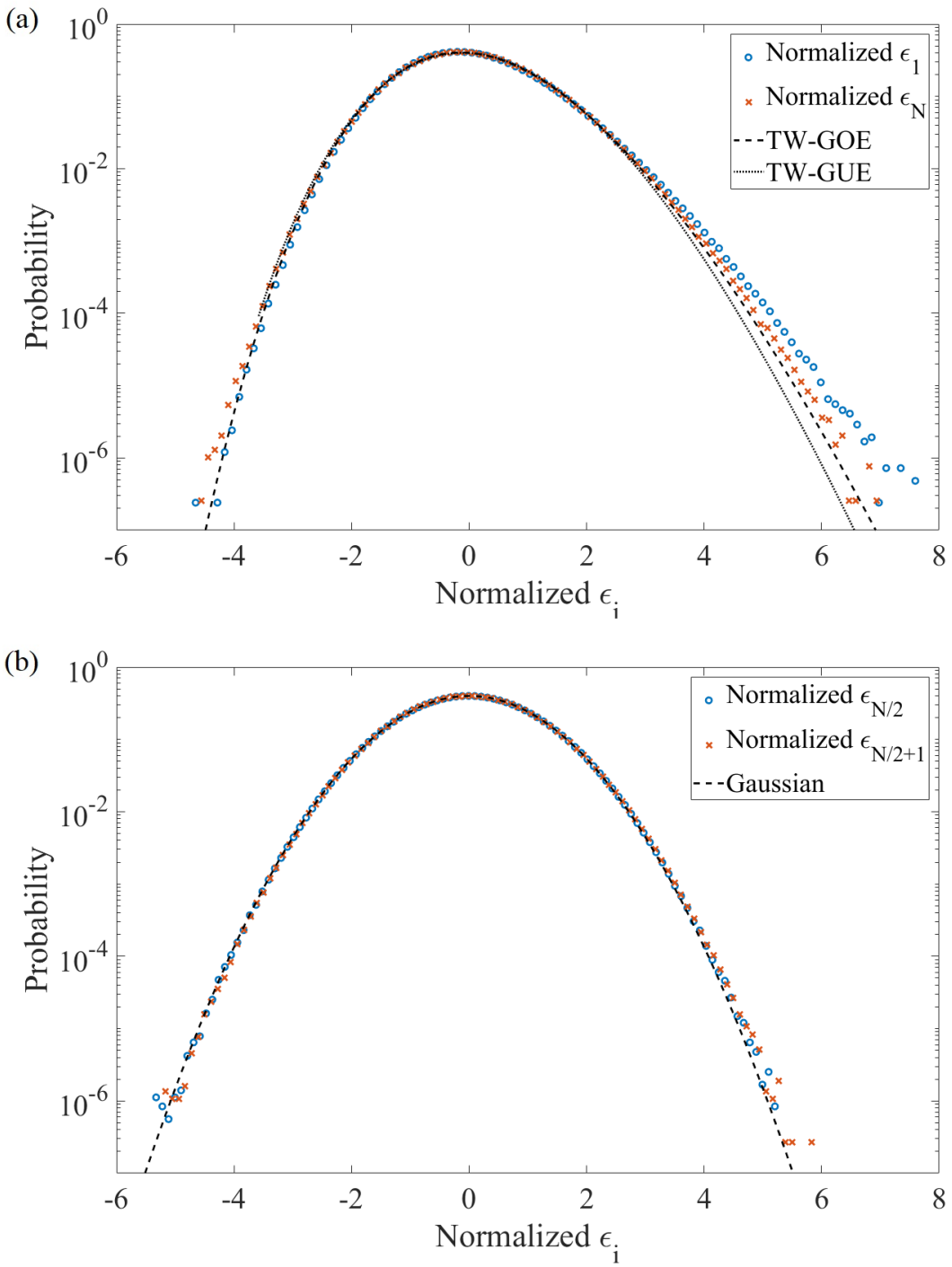

FIG. 4: Probability distribution of $\epsilon_i = \ln \lambda_i / t$ for the product of DPRM transfer matrices. All distributions are normalized to have mean 0 and variance 1. (a) On the edges of the spectrum, ϵ_1 and ϵ_N have asymmetric distributions consistent with the TW forms. (b) In contrast, ϵ_i in the bulk are Gaussian distributed, similar to the bulk eigenvalues of GOE and GUE matrices.

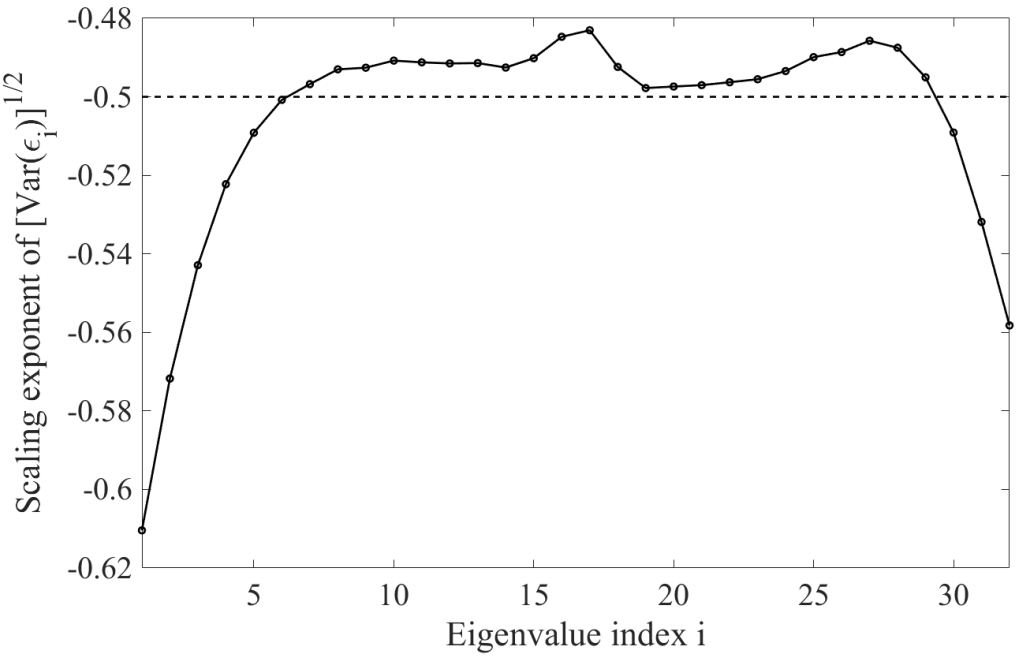

FIG. 5: Scaling exponents for the variance of $\epsilon_i = \ln \lambda_i / t$ for the product of DPRM transfer matrices. For ϵ_1, the scaling of fluctuations $[\mathrm{Var}(\epsilon_i)]^{1/2}$ is consistent with $t^{-2/3}$, expected for the DPRM free energy. For bulk ϵ_i, however, the scaling is approximately $t^{-1/2}$, similar to that of i.i.d. random variables drawn from a Wigner semicircle distribution.

although to a lesser extent.

C. Density of states

We now compare the eigenvalue spacings for the DPRM product matrix in disordered and pure systems, focusing our attention on the density of states near ϵ_1. In the pure system, the transfer matrix is time-independent, and the eigenvalues are fixed. We take $\mathbf{T}_{\mathrm{pure}}$ to be of the following form,

$$\mathbf{T}_{\mathrm{pure}} = \begin{pmatrix} \bar{\eta} & \gamma & 0 & \cdots & \gamma \\ \gamma & \bar{\eta} & \gamma & \cdots & 0 \\ 0 & \gamma & \bar{\eta} & \cdots & 0 \\ \vdots & \vdots & \vdots & \ddots & \vdots \\ \gamma & 0 & 0 & \cdots & \bar{\eta} \end{pmatrix}, \tag{16}$$

where $\bar{\eta}$ is the average strength of disorder $\eta_i(t)$ defined in Eq. 13 and 14. We have introduced additional hopping terms γ in the $(1, N)$ and $(N, 1)$ positions, which correspond to periodic boundary conditions. The effect on the spectrum is negligible for large system sizes, and the advantage of this choice is that Eq. 16 is a circulant matrix whose spectrum is known analytically,

$$\epsilon_k^{\text{pure}} = \frac{\ln \lambda_k^{\text{pure}}}{t} = \bar{\eta} + 2\gamma \cos\left[\frac{2\pi k}{N}\right], \qquad k = 0, 1, \ldots, N-1. \tag{17}$$

[Note that the eigenvalues in the above form are not ordered, and that the bulk eigenvalues (i.e. not the maximum or minimum) are degenerate.]

We plot ϵ_i for the disordered and pure DPRM systems in Fig. 6. We see that in the disordered case, the "energy band" is linear near ϵ_1, rather than quadratic. It is therefore more energetically costly to add non-intersecting directed polymers into the system. We plot also the mean eigenvalues for rescaled Gaussian random matrices for reference. (The curves for GOE and GUE matrices are indistinguishable, so only one is plotted.) There, the density of states follows the Wigner semicircle distribution, which vanishes continuously at the edge of the spectrum as $n \to \infty$.

V. TOTALLY POSITIVE MATRICES

We devote this section to proving the claim that the product of DPRM transfer matrices, as defined in Eq. 2 and 13, has eigenvalues which are all real and positive. To see this, we turn to a class of matrices known as totally positive matrices [26, 27].

We begin with some definitions. An $N \times N$ matrix $\mathbf{A} = \{a_{ij}\}_{i,j=1}^{N}$ is *totally positive* if the determinant of any square submatrix (obtained by omitting $N-k$ rows and columns) is positive. More precisely, let $\{i_l\}_{l=1}^{k}$ and $\{j_m\}_{m=1}^{k}$ be increasing subsequences of $\{1, \ldots, N\}$, with length $k < N$. Then $\mathbf{A}' = \{a_{i_l, j_m}\}_{l,m=1}^{k}$ is a square submatrix of $\mathbf{A}$. As a special case, a *minor* M_{ij} of $\mathbf{A}$ is the determinant of the submatrix obtained by removing the ith row and the jth column. Furthermore, if $i = j$, M_{ij} is called a *principal minor*. A consequence of this definition is that a totally positive matrix $\mathbf{A}$ is necessarily also *positive* (has all positive entries) and *positive-definite* (has all positive eigenvalues).

The key property we exploit is that total positivity is preserved under matrix multiplication. We begin by proving this closure property. We then verify that each individual

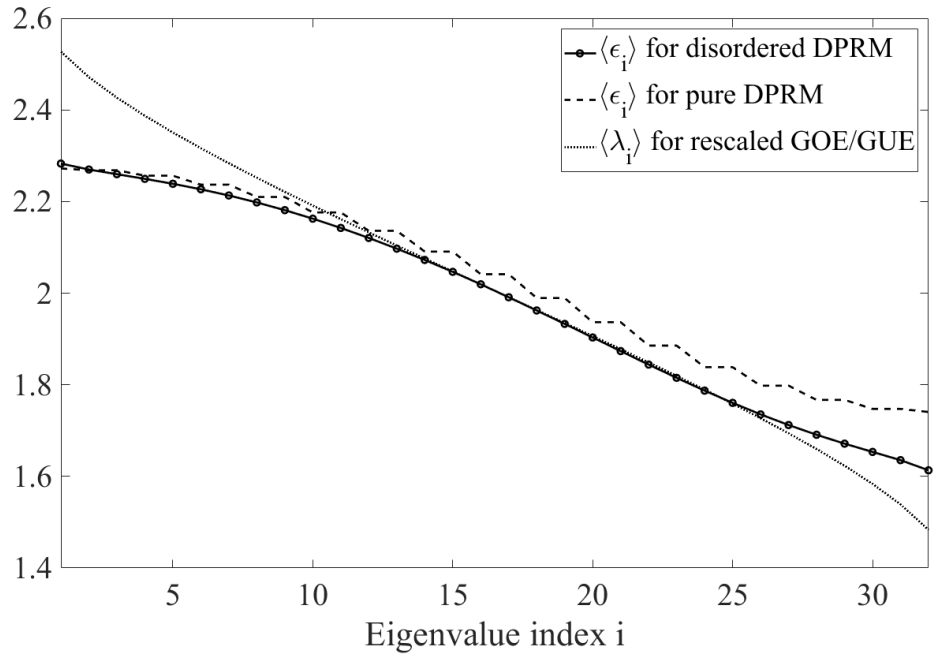

FIG. 6: ϵ_i for disordered DPRM (solid line), plotted against the analogous quantity for the pure system (dashed line), and the rescaled mean eigenvalues of Gaussian random matrices (dotted line). The "steps" in the dashed line arise from degeneracy. Near $i = 1$, the curve is linear for disordered DPRM, in contrast to quadratic for pure DPRM.

transfer matrix $\mathbf{T}$ defined in Eq. 13 is totally positive. These results combine to show that the product matrix $\mathbf{W}$ is totally positive, with real and positive eigenvalues.

A. Closure under matrix multiplication

Consider two $N \times N$ totally positive matrices $\mathbf{A}$ and $\mathbf{B}$. By the Cauchy-Binet theorem, the determinant of a $k \times k$ submatrix of the product $\mathbf{AB}$ can be written as

$$\det[(\mathbf{AB})_{\mathcal{IJ}}] = \sum_{\mathcal{H}} \det(\mathbf{A}_{\mathcal{IH}}) \det(\mathbf{B}_{\mathcal{HJ}}) \tag{18}$$

where $\mathcal{I}$, $\mathcal{J}$, and $\mathcal{H}$ are increasing subsequences of $\{1, \ldots, N\}$, with length k. The sum is over all possible such subsequences $\mathcal{H}$. Since $\mathbf{A}$ and $\mathbf{B}$ are totally positive, $\det(\mathbf{A}_{\mathcal{IH}}) > 0$ and $\det(\mathbf{B}_{\mathcal{HJ}}) > 0$ for any $\mathcal{H}$. This immediately gives $\det[(\mathbf{AB})_{\mathcal{IJ}}] > 0$ for any minor of the product $\mathbf{AB}$. Thus $\mathbf{AB}$ must also be totally positive. The argument trivially generalizes to the product of $n > 2$ matrices. Therefore, totally positive matrices are closed under matrix

multiplication.

B. Total positivity of the transfer matrix

It remains to show that the DPRM transfer matrix introduced in Eq. 13 is indeed totally positive. We rewrite Eq. 13 as

$$\mathbf{T}(t) = \mathbf{T}_0 + \mathbf{E}(t),$$

$$\mathbf{T}_0 = \gamma \begin{pmatrix} 2 & 1 & 0 & \cdots & 0 \\ 1 & 2 & 1 & \cdots & 0 \\ 0 & 1 & 2 & \cdots & 0 \\ \vdots & \vdots & \vdots & \ddots & \vdots \\ 0 & 0 & 0 & \cdots & 2 \end{pmatrix},$$

$$\mathbf{E}(t) = \begin{pmatrix} \eta_1(t) - 2\gamma & 0 & 0 & \cdots & 0 \\ 0 & \eta_2(t) - 2\gamma & 0 & \cdots & 0 \\ 0 & 0 & \eta_3(t) - 2\gamma & \cdots & 0 \\ \vdots & \vdots & \vdots & \ddots & \vdots \\ 0 & 0 & 0 & \cdots & \eta_N(t) - 2\gamma \end{pmatrix}. \tag{19}$$

$\mathbf{T}_0$ is now a time-independent Jacobi (tri-diagonal) matrix, while $\mathbf{E}(t)$ is a positive diagonal matrix due to the constraints we placed on the noise $\eta_i(t)$ in Eq. 14. To proceed, we make use of Theorem 2.3 and Corollary 2.4 from Ref. [27].

Theorem. (Ando, 1987) Let $\mathbf{A}$ be an N-square Jacobi matrix. If $\mathbf{A}$ is positive, and all principal minors are positive, then $\mathbf{A}$ is totally positive. Furthermore, for any $s_i > 0, i = 1, 2, \ldots, N$,

$$\det[\mathbf{A} + \mathrm{diag}(s_1, \ldots, s_N)] \geq \det \mathbf{A} + \sum_i s_i, \tag{20}$$

and it follows that $\mathbf{A} + \mathrm{diag}(s_1, \ldots, s_N)$ is also totally positive.

If $\mathbf{T}_0$ is totally positive, then by the above theorem, $\mathbf{T}(t) = \mathbf{T}_0 + \mathbf{E}(t)$ is totally positive $\forall t$. It is trivial that $\mathbf{T}_0$ is positive. We need only show that all principal minors are positive as well. However, if we denote the Jacobi matrix $\mathbf{T}_0$ of size N as $\mathbf{T}_0^N$, the principal minor M_{ii} of $\mathbf{T}_0^N$ can be written in terms of a block matrix,

$$M_{ii} = \det \begin{pmatrix} \mathbf{T}_0^{i-1} & \mathbf{0} \\ \mathbf{0} & \mathbf{T}_0^{N-i} \end{pmatrix} = \det(\mathbf{T}_0^{i-1}) \det(\mathbf{T}_0^{N-i}) \tag{21}$$

Thus the proof reduces to showing $\det(\mathbf{T}_0^k) > 0$, $\forall k < N$.

We write $\mathbf{T}_0^k$ as a block matrix in the following form,

$$\mathbf{T}_0^k/\gamma = \begin{pmatrix} 2 & \mathbf{C} \\ \mathbf{C}^T & \mathbf{T}_0^{k-1}/\gamma \end{pmatrix}, \qquad \mathbf{C} = \underbrace{(1,0,\ldots,0)}_{k-1 \text{ terms}}. \tag{22}$$

Then by the Schur determinant identity,

$$\begin{aligned} \det(\mathbf{T}_0^k/\gamma) &= \det(2)\det(\mathbf{T}_0^{k-1}/\gamma - \mathbf{C}^T 2^{-1}\mathbf{C}) \\ &= 2\det\left[\mathbf{T}_0^{k-1}/\gamma - \mathrm{diag}\left(\frac{1}{2},0,\ldots,0\right)\right] \\ &= 2\left(2-\frac{1}{2}\right)\det\left[\mathbf{T}_0^{k-2}/\gamma - \mathrm{diag}\left(\frac{1}{2-\frac{1}{2}},0,\ldots,0\right)\right] \\ &= 2\left(2-\frac{1}{2}\right)\cdots\underbrace{\left(2-\cfrac{1}{2-\cfrac{1}{2-\ddots}}\right)}_{k \text{ levels}}. \end{aligned} \tag{23}$$

In the second line, we can again write the matrix in square brackets as a block matrix, as in Eq. 22. Recursively applying the determinant identity k times gives the final expression in Eq. 23. It is not difficult to see that the limit of the continued fraction is

$$\lim_{m\to\infty} \underbrace{\left(2-\cfrac{1}{2-\cfrac{1}{2-\ddots}}\right)}_{m \text{ levels}} = 1^+ \tag{24}$$

and more importantly, for any m, the continued fraction is positive. Thus $\det(\mathbf{T}_0^k) > 0$, $\forall k$, and the proof is complete.

---

[1] V. Dotsenko, Europhys. Lett. **90**, 20003 (2010).

[2] P. Calabrese, P. Le Doussal, and A. Rosso, Europhys. Lett. **90**, 20002 (2011).

[3] P. Calabrese and P. Le Doussal, Phys. Rev. Lett. **106**, 250603 (2011).

[4] L. Yan, J.-P. Bouchaud, and M. Wyart, Soft Matter **13**, 5795 (2017).

[5] V. L. Pokrovski and A. L. Talapov, Phys. Rev. Lett. **42**, 65 (1979).

[6] M. Kardar, Nucl. Phys. B **290** [FS20], 582 (1987).

[7] D. A. Huse and C. L. Henley, Phys. Rev. Lett. **54**, 2708 (1985).

[8] D. S. Fisher, Phys. Rev. Lett. **56**, 1964 (1986).

[9] G. Blatter, M. V. Feigel'man, V. B. Geshkenbein, A. I. Larkin, and V. M. Vinokur, Rev. Mod. Phys. **66**, 1125 (1994).

[10] M. Jaubert, A. Glachant, M. Bienfait, and G. Boato, Phys. Rev. Lett. **46**, 1679 (1981).

[11] K. Kern, R. David, P. Zeppenfeld, R. Palmer, and G. Comsa, Solid State Commun. **62**, 391 (1987).

[12] A. R. Kortan, A. Erbil, R. J. Birgeneau, and M. S. Dresselhaus, Phys. Rev. Lett. **49**, 1427 (1982).

[13] C. Rottman and M. Wortis, Phys. Rep. **103**, 59 (1984).

[14] C. Rottman, M. Wortis, J. C. Heyraud, and J. J. Métois, Phys. Rev. Lett. **52**, 1009 (1984).

[15] S. N. Coppersmith, D. S. Fisher, B. I. Halperin, P. A. Lee, and W. F. Brinkman, Phys. Rev. B **25**, 349 (1982).

[16] M. E. Fisher and D. S. Fisher, Phys. Rev. B **25**, 3192 (1982).

[17] J. Villain, Journal de Physique Lettres, **43**, 551 (1982).

[18] T. Halpin-Healy and Y.-C. Zhang, Phys. Rep. **254**, 215 (1995).

[19] C. A. Tracy and H. Widom, Commun. Math. Phys. **177**, 727 (1996).

[20] C. A. Tracy and H. Widom, ICM **I**, 587 (2002).

[21] E. P. Wigner, Ann. Math. **67**, 325 (1958).

[22] J. Gustavsson, Annales de l'I.H.P. Probabilités et statistiques **41**, 151 (2005).

[23] S. O'Rourke, J. Stat. Phys. **138**, 1045 (2010).

[24] L. Erdős, H.-T. Yau, and J. Yin, Adv. Math. **229**, 1435 (2012).

[25] F. Benaych-Georges and A. Knowles, arXiv:1601.04055 (2016).

[26] C. Loewner, Mathematische Zeitschrift **63**, 338 (1955).

[27] T. Ando, Linear Algebra Appl. **90**, 165 (1987).